A computational model of cochlear nucleus neurons

Katuhiro Maki[1] and Masato Akagi[2]

[1] Human and Information Science Laboratory, NTT Communication Science Laboratories, NTT Corporation, maki@avg.brl.ntt.co.jp
[2] School of Information Science, Japan Advanced Institute of Science and Technology, akagi@jaist.ac.jp

1 Introduction

The cochlear nucleus (CN), the first processing center in the auditory central nervous system, consists of diverse neuronal types that differ in their patterns of temporal response to short tone bursts (Blackburn and Sachs 1989). Several functional models have been proposed and have demonstrated some degree of success in simulating the temporal response patterns of CN neurons (Arle and Kim 1991; Banks and Sachs 1991; Hewitt and Meddis 1993; Cai, Walsh and McGee 1997; Levy and Kipke 1997; Eriksson and Robert 1999). Those models, however, involve solving systems of differential equations based on the Hodgkin-Huxley equation (Hodgkin and Huxley 1952) and therefore tend to have complex structures and many parameters (typically ≥ 10). A simple model with relatively few parameters would be useful not only for future implementation in a large-scale computer simulation, but also for estimating the underlying mechanisms generating the response of CN neurons to a variety of complex sounds, such as vocalizations. In this paper, we propose a model that represents the synaptic transduction mechanisms and membrane properties with stochastic processes. The model is expressed with only eight parameters. By fitting appropriate parameter values, the model can successfully simulate various temporal response types found in the anteroventral CN (AVCN), such as the primary-like (with or without notch), the chopper (regular and irregular), and the onset types, as well as the degree of phase-locking and response latencies.

2 Model

The input to the model is a train of discrete pulses that simulates inputs from multiple auditory nerve fibers (ANFs). The arrival time of the jth pulse in the train of pulses from the ith ANF input is denoted by t_{ij}. The post-synaptic potential (PSP) of a CN neuron at time t is modeled by:

$$V(t) = \sum_{i=1}^{N} \sum_{\{j|t_{ij}+t_c<t\}} a_i(t - t_c - t_{ij})\, e^{-(t-t_c-t_{ij})/\tau_i} \tag{1}$$

where N($\in \mathbf{Z}^+$) is the total number of input pulses, and t_c is random jitter from the normal distribution with a mean μ_c and a variance ${\sigma_c}^2$ ($t_c \sim N\left(\mu_c, {\sigma_c}^2\right)$). The values of μ_c and σ_c, respectively, determine the response latency and the degree of phase-locking of the CN neurons. The $\tau_i (\in \mathbf{R}^+)$ is the time constant of a PSP elicited by a single input pulse. The a_i is a coefficient of synaptic strength that determines the magnitude of PSP elicited by a single pulse input. A positive a_i indicates that the input is excitatory, and a negative a_i that it is inhibitory.

The output S at time t is represented by,

$$S(t) = \begin{cases} 1 & V(t) \stackrel{\geq}{=} U(\alpha, \beta) \text{ and } S(t') = 0 \text{ for } t' \in [t - t_r, t], \\ 0 & \text{otherwise.} \end{cases} \tag{2}$$

The output of the modeled neuron is a train of all-or-none (1 or 0) action potentials with unit amplitudes. Action potentials of the model are generated when the membrane potential V crosses a threshold U. The threshold U is a random variable from a uniform distribution in the range from α to β. The modeled neuron does not generate a spike during the refractory period after the previous spike. Refractory period t_r is modeled by a random variable from a normal distribution with a mean μ_r and a variance ${\sigma_r}^2$ ($t_r \sim N\left(\mu_r, {\sigma_r}^2\right)$).

3 Methods of evaluation

Figure 1 shows classification results for actual AVCN units (Blackburn and Sachs 1989). The model was evaluated with respect to its ability to reproduce the temporal response patterns in Fig. 1 and phase-locking properties of actual AVCN units. As in physiological experiments (Blackburn and Sachs 1989), two stimulus durations were used in this study: short tone bursts (STBs) of 25 ms duration with 1.6 ms rise and fall times; and long tone bursts (LTBs) of 400 ms duration with 10 ms rise and fall times. Post-stimulus time histograms (PSTHs) and first-spike latency histograms were computed based on 200 presentations of the STBs at the best frequency (BF), and were represented with 0.2 ms time bins. In evaluating PSTHs, the BF of the modeled CN neuron was fixed at 4.8 kHz. All simulations were run at a sampling rate of 48 kHz.

3.1 Inputs to the modeled CN neurons

Inputs of the modeled CN neuron, i.e., discrete pulse trains, were simulated responses of ANFs at the BF of the modeled CN neuron, produced by an auditory peripheral model (Maki, Akagi and Hirota 1998). Temporal response patterns and phase-locking properties of simulated AN responses used as inputs to the modeled CN neurons are shown in Figs. 2(a) and 2(b), respectively.

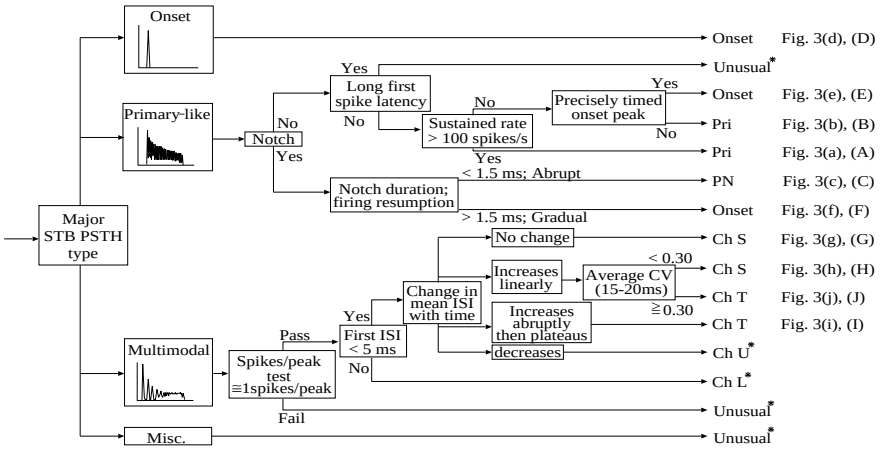

Fig. 1. Classification scheme proposed by Blackburn and Sachs for categorizing AVCN units (Blackburn and Sachs 1989). Graphs (*lefthand column*) depict major PSTH categories from which defined populations are refined. "Primary-like" PSTHs resemble those of auditory nerve fibers (ANFs). "Onset" PSTHs have a sharp peak at stimulus onset, followed by little or no sustained activity. Units are placed in the "onset" limb only if their sustained rates are $\leq$ 25 spikes/s. "Chopper" PSTHs have regularly spaced peaks of discharge whose period is not related to the stimulus frequency. Response types discarded in the study of Blackburn and Sachs (*) were also excluded in present study.

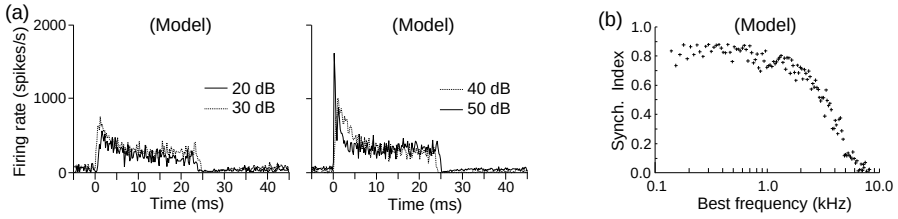

Fig. 2. Temporal response patterns and phase-locking properties of inputs to the CN model. (a) PSTHs of simulated ANF for five stimulus levels (20, 30, 35, 40 and 50 dB). PSTHs are represented with 0.2-ms time bins. (b) Synchronization index (Goldberg and Brown 1969) of simulated AN firing as a function of BF.

In Fig. 2(a), PSTHs calculated from the simulated ANF firing show temporal properties similar to actual ANFs (Johnson 1980). That is, there is an initial rapid increase of firing rate at the response onset, which strongly depends on the stimulus level, followed by a sustained discharge at a lower spike rate during stimulation. The simulated ANF responses show that the degree of phase-locking to BF tones decreases gradually with BF in the range from 0.1 to 1.5 - 2.0 kHz, and then drops sharply to reach the noise level above 5.0 - 6.0 kHz. This tendancy is also observed in actual ANFs (Johnson 1980).

4 Results

We adjusted the parameters of the CN model and selected the CN model inputs (i.e., simulated AN responses in Fig. 2) so that the CN model simulates the ten kinds of response patterns in Fig. 1. The parameter values used in this study are summarized in Table 1.

Table1. The parameter of the CN model for simulating each response type. "N" shows the total number of simulated AN inputs. "dB" indicates the stimulus sound level. Important parameter boundaries for differentiating the response types are indicated by vertical lines.

Type (Fig.)	Pri (3A)	Pri (3B)	PN (3C)	Onset (3D)	Onset (3E)	Onset (3F)	Ch S (3G)	Ch S (3H)	Ch T (3I)	Ch T (3J)
a_i	1	1	1	1	1	1	1	1	1	1
τ_i ([value]$\times 10^{-6}$)	6.7	6.7	4.8	6.7	4.8	4.8	11	25	66	50
μ_c (s)	0.005	0.005	0.005	0.005	0.005	0.005	0.005	0.005	0.005	0.005
σ_c ([value]$\times 10^{-5}$ s)	5	5	4	5	5	4	17	14	16	15
μ_r ([value]$\times 10^{-4}$s)	8	8	12	15	16	30	18	21	13	16
σ_r ([value]$\times \mu_r$ s)	0.050	0.025	0.025	0.025	0.003	0.230	0.025	0.025	0.025	0.040
β ([value]$\times 10^{-6}$)	5.38	7.69	2.81	3.09	2.13	0.90	12.9	18.0	243	153
α ([value]$\times 10^{-6}$)	0.84	1.00	0.17	2.75	0.49	0.57	2.29	18.0	96.0	33.3
N	30	30	30	50	50	65	50	30	50	30
dB	20	30	50	50	50	50	50	45	40	40

4.1 Response types

The simulation results for the CN model are shown in Figs. 3(A)-(J). Comparable physiological data are shown in Figs. 3(a)-(j). All the responses of the model meet the classification requirements of the decision tree in Fig. 1. The modeled and actual Pri units both have a broad distribution of first-spike latency, in contrast to other response types, which show a restricted distribution [(A) and (a), (B) and (b)]. PSTHs of both modeled and actual PN units show a firing notch after the initial response peak [(C) and (c)]. The three modeled Onset units shown in (D), (E) and (F) differ in pattern after the initial response peak as found in actual Onset units [(d), (e), and (f)]. That is, the unit in (D) shows essentially no firing ($<$ 25 spikes/s) after the onset response; the unit in (E) shows slight sustained firing ($\geq$25 spikes/s and $<$100 spikes/s); the unit shown in (F) has a firing notch at around 6 ms. The data in (G)-(J) and (g)-(j) indicate that PSTHs of the two Ch S and two Ch T units modeled agree with the physiological data in the number of regular spaced peaks for the first 10 ms after the response onset. The modeled and the actual Ch S unit in (G) and (g) have a mean inter-spike interval (ISI) that is nearly constant throughout the entire response to the STB [(G') and (g')]. Similar to the actual Ch T unit in (i), the modeled Ch T unit in (I) has a mean ISI that stabilizes after the initial transient response [(I')]. Both the actual Ch T and Ch S units in (h) and (j) have a mean ISI that increases more or less linearly with time for the first 15 ms of the response to STB. The difference between these two units is in the average CV (Young, Robert and Shofner 1988, see caption of Fig. 3) between 15-20 ms after the response onset, i.e., the Ch T unit has larger average CV than the Ch S unit. These characteristics are also found in the modeled Ch T and Ch S units in (H) and (J).

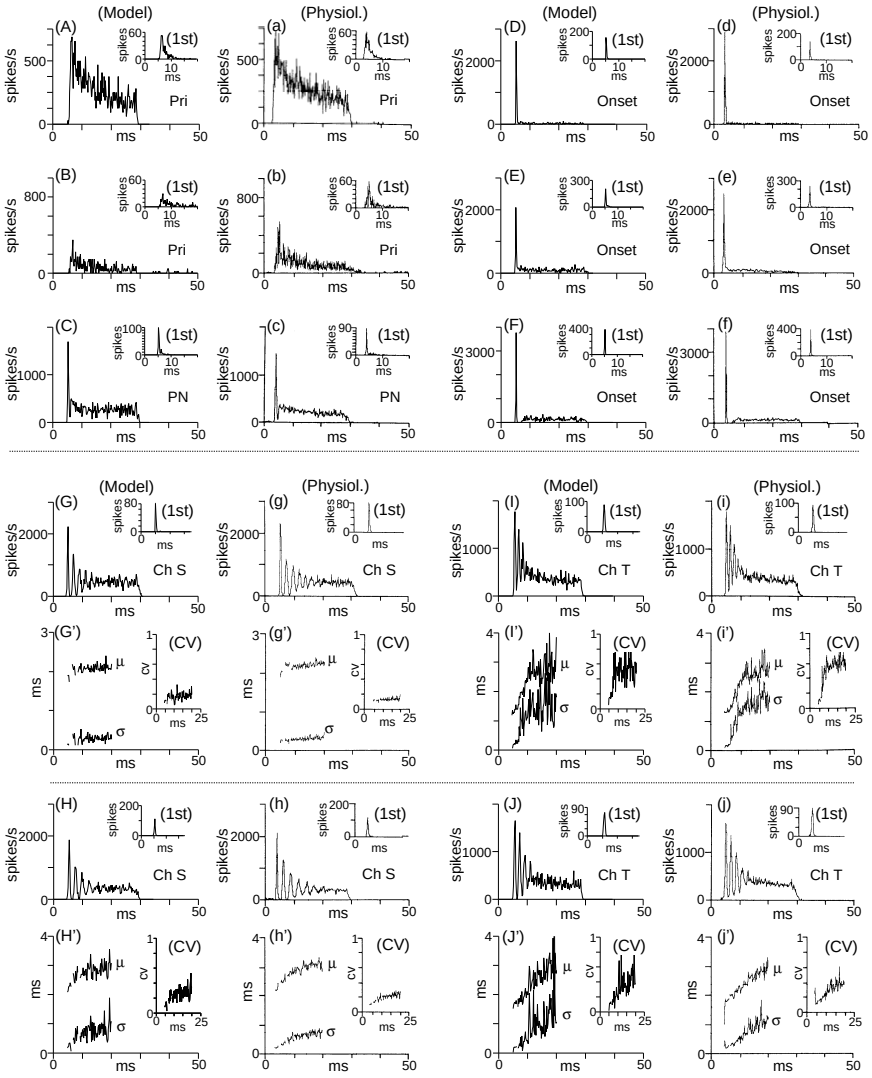

Fig. 3. Temporal properties of modeled and actual CN units' responses to STBs. (Model) Data from the model. (Physiol.) Physiological data redrawn from the original paper (Blackburn and Sachs 1989). Response types are indicated at right bottom in each PSTH figure. First-spike latency histograms (1st) are shown in the insets. The time scale for the first-spike latency is the same as that for PSTH. (G')-(J'), (g')-(j') The μ and σ respectively indicate the mean and standard deviation of inter-spike interval of spike data shown above (PSTH) (regularity analysis; Young, *et al* 1988). CV is calculated by dividing σ by μ (Young, *et al* 1988).

4.2 Phase-locking properties

The synchronization index (Goldberg and Brown 1969) calculated for individual response types of the model in response to a BF tone are plotted as a function of BF in

Fig. 4(a) and (b), where the lines indicate least-squares fits to actual Pri and PN units data, and actual Ch S and Ch T units data, respectively (Blackburn and Sachs 1989).

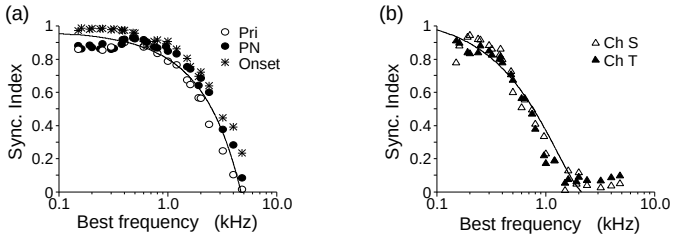

Fig. 4. Synchronization index of modeled responses as a function of BF. Dots represent data from the model. Lines in (a) and (b) indicate second-order polynomial functions fit to actual primary-like (Pri and PN) and chopper (Ch S and Ch T) units data, respectively, by use of least-squares (Blackburn and Sachs 1989). As in the case of the physiological data, calculations for the model were based on the entire response (10-400 ms) to a 400-ms long tone burst.

The pattern of the BF dependency of the phase-locking for the actual Pri and PN units resemble those for the ANFs [see Fig. 2(b)] in the fall-off of synchronization with increasing frequency between 1 and 5 kHz. The degree of phase-locking of actual Ch T and Ch S units falls more rapidly as a function of BF than does that of the Pri and PN units, approaching the noise level for BF $>$ 1.5-2.5 kHz. The phase-locking degree of the two modeled primary-like units (Pri and PN) and two chopper units (Ch S and Ch T) closely follows the polynomial curve fit to the degree of phase-locking in actual CN units. Similarly to the actual Onset units, the modeled Onset units show a phase-locking ability resembling that of the Pri and PN units.

5 Discussion

We examined the eight parameters of the CN model and two parameters of the model inputs shown in Table 1, and found that only five of them are relevant for differentiating the response types. The two chopper (Ch S and Ch T) units modeled need a larger time constant of the PSPs (τ_i) than Pri, PN and Onset units. The modeled Ch T units have higher firing thresholds (α and β) than the modeled Ch S units. Consequently, the modeled Ch T units show more irregular discharge than the modeled Ch S units. Parameter values for the two primary-like units (Pri and PN) and Onset units are similar, except that Onset units receive a relatively larger number of inputs from the simulated ANFs (parameter N) and have a slightly higher firing threshold (α) than the primary-like units. The values of parameter σ_c determine the decay curves of phase-locking in Fig. 4. For a larger value of σ_c, the ability of the modeled CN neurons to phase-lock to BF tones falls more rapidly as a function of BF.

6 Conclusion

We proposed a computational model that functionally models the firing mechanisms of CN neurons. The model consists of eight parameters. We compared the responses of the model with physiological data from the AVCN (Blackburn and Sachs 1989), and found that the model could successfully simulate all temporal response types in term of the PSTHs, the degree of phase-locking, and spike latencies. Since the assumptions adopted are simple and are not specific to CN neurons, the proposed model can be easily extended to model neurons in higher-level auditory nuclei.

Acknowledgments

The authors thank Dr. Shigeto Furukawa for very helpful comments on an earlier version of this manuscript.

References

Arle, J.E. and Kim, D.O. (1991) Neural modeling of intrinsic and spike-discharge properties of cochlear nucleus neurons. Biol. Cybern. 64, 273-283.

Banks, M.I. and Sachs, M.B. (1991) Regularity analysis in a compartmental model of chopper units in the anteroventral cochlear nucleus. J. Neurophysiol. 65, 606-629.

Blackburn, C.C. and Sachs, M.B. (1989) Classification of unit types in the anteroventral cochlear nucleus: Histograms and regularity analysis. J. Neurophysiol. 62, 1303-1329.

Cai, Y., Walsh. E.J. and McGee, J. (1997) Mechanisms of onset responses in octopus cells of the cochlear nucleus: Implications of a model. J. Neurophysiol. 78, 872-883.

Eriksson, J.L., Robert, A. (1999) The representation of pure tones and noise in a model of cochlear nucleus neurons. J. Acoust. Soc. Am. 106, 1865-1879.

Goldberg, J.M. and Brown, P.B. (1969). Response of binaural neurons of dog superior olivary complex to dichotic tonal stimuli: Some physiological mechanisms of sound localization. J. Neurophysiol. 32, 613-636.

Hewitt, M.J. and Meddis, R. (1993) Regularity of cochlear nucleus stellate cells: A computational modeling study. J. Acoust. Soc. Am. 93, 3390-3399.

Hodgkin, A.L. and Huxley, A.F. (1952) A quantitative description of membrane current and its application to conduction and excitation in nerve. J. Physiol. 117, 500-544.

Johnson, D.H. (1980) The relationship between spike rate and synchrony in responses of auditory-nerve fibers to single tones. J. Acoust. Soc. Am. 68, 1115-1122.

Levy, K.L. and Kipke, D.R. (1997) A computational model of the cochlear nucleus octopus cell. J. Acoust. Soc. Am. 102, 391-402.

Maki, K., Akagi, M. and Hitota, K. (1998) A functional model of the auditory peripheral system: Responses to simple and complex stimuli. Proc. of NATO/ASI Computational Hearing Conference, 13-18.

Westerman, L.A., and Smith, R.L. (1984) Rapid and Short Term Adaptation in Auditory-Nerve Responses. Hear. Res. 15, 249-260.

Young, E.D., Robert, J.M. and Shofner, W.P. (1988) Regularity and latency of units in ventral cochlear nucleus: Implications for unit classification and generation of response properties. J. Neurophysiol. 60, 1-29.